

RESEARCH

Open Access



Maximizing oxaliplatin's impact on EGFR⁺ colorectal cancer through targeted extracellular vesicles

Shang-Tao Chien^{1,2†}, Yi-Jung Huang^{3,4†}, Ming-Yii Huang^{5,6,7}, Yi-Ping Fang^{8,9,10}, Shi-Wei Chao¹¹, Chia-Tse Li¹¹, Wun-Ya Jhang¹¹, Yun-Han Hsu¹¹, Shuo-Hung Wang¹¹ and Chih-Hung Chuang^{4,11*}

[†]Shang-Tao Chien and Yi-Jung Huang have contributed equally.

*Correspondence: a4132600@gmail.com

⁴Drug Development and Value Creation Research Center, Kaohsiung Medical University, Kaohsiung, Taiwan
Full list of author information is available at the end of the article

Abstract

Purpose: To investigate the ability of extracellular vesicles (EVs) to deliver oxaliplatin to epidermal growth factor receptor (EGFR⁺) colorectal cancer cells and increase oxaliplatin's cytotoxicity.

Method: Oxaliplatin was passively loaded into a stable cell line expressing cetuximab in membranes. EVs were collected and characterized for size, and their ability to target EGFR⁺ cells was tested. Cytotoxicity experiments were performed, and a xenograft cancer animal model was used to confirm the specific accumulation of oxaliplatin-loaded EVs with cetuximab-expressing membranes in EGFR⁺ cells.

Results: EVs with cetuximab-expressing membranes were successfully produced and used to encapsulate oxaliplatin, resulting in consistently sized oxaliplatin-loaded EVs with cetuximab-expressing membranes. The oxaliplatin-loaded EVs with cetuximab-expressing membranes were specifically accumulated by EGFR⁺ cells, leading to significant cytotoxic effects on these cells. In the animal model, the oxaliplatin-loaded EVs with cetuximab-expressing membranes accumulated specifically in EGFR⁺ cells and significantly enhanced oxaliplatin's therapeutic efficacy against EGFR⁺ cancer cells.

Conclusion: EVs with membrane-expressed bioactive molecules are a promising strategy for delivering therapeutic agents to EGFR⁺ colorectal cancer cells.

Highlights

1. EVs with cetuximab-expressing membranes were used to encapsulate oxaliplatin and target EGFR⁺ cells.
2. Oxaliplatin-loaded EVs with cetuximab-expressing membranes exhibited significant cytotoxic effects on EGFR⁺ cells.
3. In a xenograft cancer animal model, oxaliplatin-loaded EVs with cetuximab-expressing membranes accumulated specifically in EGFR⁺ cells and significantly enhanced oxaliplatin's therapeutic efficacy against EGFR⁺ cancer cells.



4. EVs with targeted membrane expression of drugs are a promising strategy for delivering therapeutic agents to specific cell populations.

Keywords: Extracellular vesicles, Oxaliplatin delivery, EGFR⁺ colorectal cancer

Introduction

Extracellular vesicles (EVs) are secreted by the cells themselves, which makes them biocompatible. Compared to synthetic drug carriers, EVs undergo more natural excretion and metabolism processes in the body. In addition, EVs can reduce interactions with the immune system, thereby mitigating potential immune reactions. These characteristics make them excellent carriers for the delivery of therapeutic drugs (Zeng et al. 2022; Zhang et al. 2020; Fu et al. 2021; Kooijmans et al. 2016a). For example, Somiya et al. demonstrated excellent biocompatibility of EVs in vivo, as they were cleared without adverse reactions. The toxicity, immunology, and immunogenicity of EVs have also been evaluated, with results showing acceptable biocompatibility in vivo (Somiya et al. 2018). Wu et al. highlighted that EVs, being products of endogenous secretion, exhibit good biocompatibility within the body and can reduce interactions with the immune system. These attributes confer potential advantages to EVs as drug delivery systems and mitigate the risk of immune reactions (Wu et al. 2021).

Targeting the specificity of EVs is crucial for their application in disease treatment. For instance, Zhu et al. demonstrated that conjugated Hypo-Exo with an ischemic myocardium-targeted peptide facilitates ischemic cardiac repair by ameliorating cardiomyocyte apoptosis. This indicates that particular peptides can enable EVs to acquire targeted specificity (Zhu et al. 2018). In breast cancer treatment, the targeting of EVs using anti-human CD3 and anti-human HER2 antibodies has been employed to generate SMART-Exos that dual-target T cells to CD3 and HER2 receptors associated with breast cancer. This approach enhances the efficacy of targeting of HER2-positive breast cancer cells by T cells (Tian et al. 2023; Chen et al. 2024; Rahbarghazi et al. 2019; Chang et al. 2021; Hou et al. 2023; Liu et al. 2023). In lung cancer treatment, ligands that bind to the epidermal growth factor receptor (EGFR) can be modified to attach to the surface of EVs to increase their binding and uptake by EGFR-positive tumor cells. In previous studies, EVs have been co-incubated with epidermal growth factor or EGFR antibodies to allow the ligands to bind to the EV surface and the targeted effects of the modified EVs on tumor cells have been evaluated using cell-based assays and animal models (Stridfeldt et al. 2023; Kooijmans et al. 2016b; Li et al. 2018; Shi et al. 2020; Cheng et al. 2018; Chao et al. 2012). Although targeted EVs have been applied in breast cancer and lung cancer, their application in colorectal cancer remains unclear.

In this study, we passively loaded oxaliplatin into a stable cell line expressing cetuximab, an EGFR inhibitor, in the membrane and collected its EVs to confirm their ability to load oxaliplatin and target EGFR to increase the cytotoxicity of oxaliplatin in EGFR⁺ colorectal cancer cells (Fig. 1, top). We constructed EVs able to express cetuximab on the membrane and then confirmed cetuximab expression on the EV membrane. We also confirmed whether the EVs changed their particle size after encapsulating oxaliplatin. We investigated whether EVs with cetuximab-expressing membranes could be accumulated by EGFR⁺ colorectal cancer cells to increase cytotoxicity. Finally,

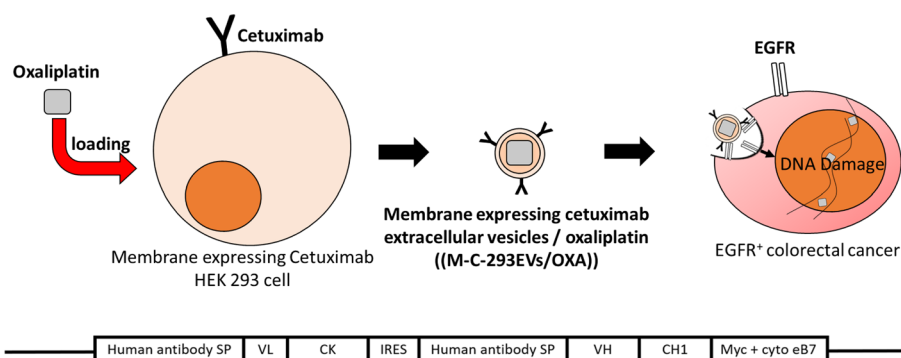


Fig. 1 Schematic diagram of the membrane-expressing cetuximab extracellular vesicles inducing cytotoxicity in EGFR+ colorectal cancer. Passively load oxaliplatin into a stable cell line expressing anti-EGFR antibodies in the membrane to produce extracellular vesicles that form membrane-expressing anti-EGFR antibody extracellular vesicles/oxaliplatin (M-C-293EVs/OXA). This would increase the toxicity of EGFR+ colorectal cancer (top). M-C-293EVs contain the cetuximab light chain variable region (VL), light chain constant region kappa (CK), internal ribosome entry site (IRES), heavy chain variable region (VH), heavy chain constant region 1 (CH1), myc tag epitope (EQKLISEEDL), and cyto eB7, which allows antibody fragments to be expressed on the membrane (bottom)

we established a xenograft colorectal animal model to confirm the tumor-specific accumulation of oxaliplatin-encapsulating EVs with cetuximab-expressing membranes and their therapeutic effect on EGFR⁺ colorectal cancer.

Results

To characterize the molecules, antibodies, and average particle size of the membranes from M-C-293EVs and M-C-293EVs/OXA

To produce extracellular vesicles (EVs) expressing cetuximab on their membranes, we constructed a plasmid on the pLKO_AS2 vector (Fig. 1, bottom) by combining human antibody messenger sequences for the light and heavy chains of cetuximab, along with CH1, MYC, and eB7 regions. This plasmid was then transfected into HEK293 cells to generate M-C-293 cell lines. After 48 h, we collected both cell pellets and EVs, and detected human Fab, Hsp70, CD81, and CD9. Compared to 293 cells and their EVs, clear bands were observed in both M-C-293 cells and their EVs, indicating successful establishment of cetuximab-expressing cell lines and EVs. Furthermore, EVs from M-C-293 cells exhibited distinct bands for CD81 and CD9 compared to cells, confirming the collection of EVs (Fig. 2A). To confirm the abundant expression of cetuximab on M-C-293EVs, we further analyzed them using CD9 Exosome Capture Beads. We labeled 2 mg each of 293EVs and M-C-293EVs with CD9 Exosome Capture Beads, followed by staining with Anti-Human IgG (Fab specific)-FITC antibody and fluorescence detection via flow cytometry. Results showed no difference in size or complexity, with FITC fluorescence signals at 2.2% for 293EVs and 79.3% for M-C-293EVs (Fig. 2B), indicating high antibody expression on M-C-293EV membranes. To verify the ability of M-C-293EVs to encapsulate OXA and characterize their particle size, we collected 293EVs, M-C-293EVs, and OXA-loaded M-C-293EVs (M-C-293EVs/OXA) for analysis using transmission electron microscopy and Nanoparticle Tracking Analyzer. Particle sizes were measured at 140.4, 142, and 152 nm, respectively (Fig. 2C); and with averages of 140.4 ± 0.9 nm, 142.4 ± 1.2 nm, and 152.8 ± 1.4 nm (Fig. 2D). This demonstrates that

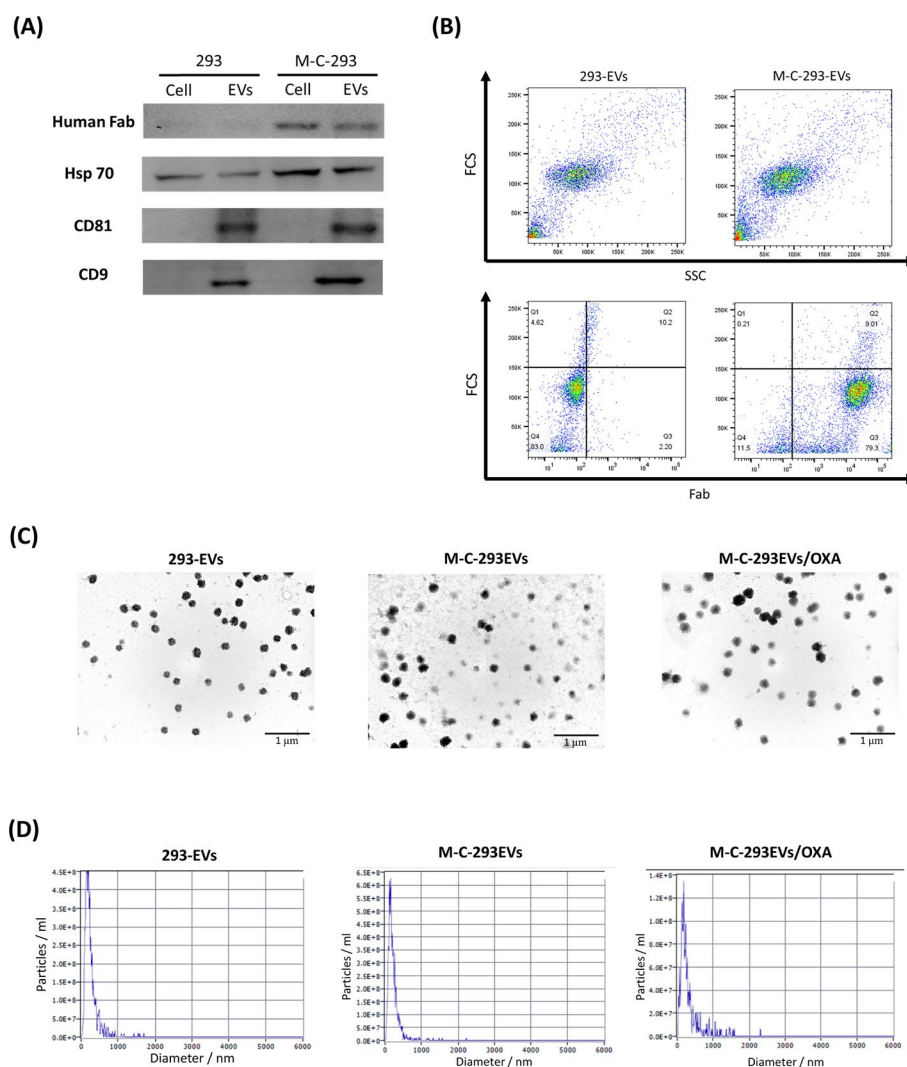


Fig. 2 Characterization of M-C-293EVs and M-C-293EVs/OXA. 30 μg of HEK293 and HEK293 cytoplasmic pellets expressing cetuximab, along with extracellular vesicles (293EVs and M-C-293EVs) were collected, and human Fab, Hsp 70, CD81, and CD9 were detected using specific antibodies (**A**). CD9 exosome capture beads labeled with 293-EVs and M-C-293EVs/OXA were stained with anti-Human IgG (Fab specific)-FITC antibody and analyzed by flow cytometry for particle size and complexity (**B**, upper panel) and human Fab expression on the EV membrane (**B**, lower panel). 20 ng of 293-EVs, M-C-293EVs, and M-C-293EVs/OXA were placed on copper grids, stained with uranyl acetate, examined by transmission electron microscopy (**C**), and analyzed for average particle size (**D**) using a Nanoparticle Tracking Analyzer. 293: HEK293 cell line; M-C-293: HEK293 cell line with cetuximab-expressing membrane; EVs: extracellular vesicles; M-C-293EVs: extracellular vesicles with cetuximab-expressing membrane; M-C-293EVs/OXA: M-C-293EVs encapsulating oxaliplatin

both antibody expression on membranes and OXA loading do not significantly alter EV integrity or size.

Following confirmation of EV integrity, we quantified OXA content in M-C-293EVs. After passive loading with 10 mg of OXA into M-C-293EVs cells for 24 h, we collected 5 mg each of M-C-293EVs and M-C-293EVs/OXA for analysis. Liquid chromatography–triple quadrupole mass spectrometry (LC–Q MS) revealed a peak at 1.71 min in M-C-293EVs/OXA (SF1C), matching the OXA standard (SF1A), while absent in M-C-293EVs (SF1B). Additionally, 5 mg/ml of M-C-293EVs/OXA contained 1.471 μg of OXA, with

encapsulation efficiency and loading capacity calculated at 0.98% and 1.471%, respectively. These results confirm successful construction of M-C-293EVs expressing cetuximab and demonstrate effective loading of OXA to form M-C-293EVs/OXA.

M-C-293EVs can specifically accumulate in EGFR + colorectal cancer cells

To confirm the specific accumulation of M-C-293EVs in EGFR + colorectal cancer cells, we loaded Rhodamine into M-C-293EVs via electroporation to create M-C-293EV/Rho. Subsequently, we applied 1, 2, and 5 mg/ml of M-C-293EV/Rho to HCT116 (EGFR+) and SW620 (EGFR-) cells for 60 min. After staining with DAPI, we detected Rhodamine and DAPI signals using fluorescence microscopy. The results showed that the signal intensity of the 5 mg/ml M-C-293EV/Rho group was higher than that of the other dosages (SF2A, 2B), particularly in HCT116 cells compared to SW620 (SF2A), indicating a dose-dependent effect of M-C-293EV/Rho. Further confirmation of M-C-293EV/Rho accumulation in EGFR + colorectal cancer cells involved treating HCT116 and SW620 cells separately with 2 mg/ml of M-C-293EVs/Rho for 60 min, followed by DAPI staining. Using confocal microscopy to detect Rhodamine, CMFDA, and DAPI signals, we observed that HCT116 cells accumulated more Rhodamine (red fluorescence) overlapping with CMFDA (green fluorescence), producing orange fluorescence (Fig. 3A), compared to SW620 (Fig. 3B). This demonstrated the specific accumulation capability of M-C-293EV/Rho in HCT116 (EGFR+) cells.

M-C-293EVs/OXA enhance the cytotoxicity against EGFR + colorectal cancer

To confirm the specific enhancement of cytotoxicity against HCT116 (EGFR+) cells by M-C-293EVs/OXA, we incubated cells with 0.1, 0.2, 0.3, 0.4, and 0.5 mg/ml of 293EVs, 293EVs/OXA, M-C-293EVs, and M-C-293EVs/OXA. After 1 h of incubation, the culture medium was replaced with fresh medium and further incubated for 48 h. Cell viability was analyzed using ATP lite assay, revealing IC₂₅ values for HCT116 of >0.5 µg/ml, >0.5 µg/ml, 0.13 µg/ml, and 0.042 µg/ml, respectively (Fig. 4A). In contrast, IC₂₅ values for SW620 were all greater than 0.5 µg/ml (Fig. 4B), demonstrating that M-C-293EVs/OXA specifically accumulate in HCT116 cells and induce cytotoxicity. Additionally, to assess the toxicity of 293EVs on normal cells, we treated WI-38, HEUVC, and PBMC with 0.1, 0.2, 0.3, 0.4, and 0.5 mg/ml of 293EVs for 48 h. Cell viability analysis showed IC₂₅ values greater than 0.5 µg/ml in all tested normal human cells, indicating that 293EVs do not induce significant toxicity in normal cells (SF3).

M-C-293EVs/Rho can specifically accumulate in EGFR + colorectal cancer in vivo

To confirm that M-C-293EVs can specifically accumulate in EGFR + colorectal cancer in mice, we injected SW620 cells into the left leg and HCT116 cells into the right leg of mice to grow tumors of approximately 50 mm³. Rhodamine was loaded into 293EVs and M-C-293EVs using electroporation to create 293EVs/Rho and M-C-293EVs/Rho. Mice were administered 2 mg/kg of either 293EVs/Rho or M-C-293EVs/Rho via tail vein injection. Fluorescence intensity at a wavelength of 580 nm was measured at 0, 30, 120, 180, and 240 min post-injection. The results showed that the fluorescence intensity in both SW620 and HCT116 tumor sites for the 293EVs/Rho group did not exceed 0.6×10^9 at any time point (Fig. 5A). In contrast, for the

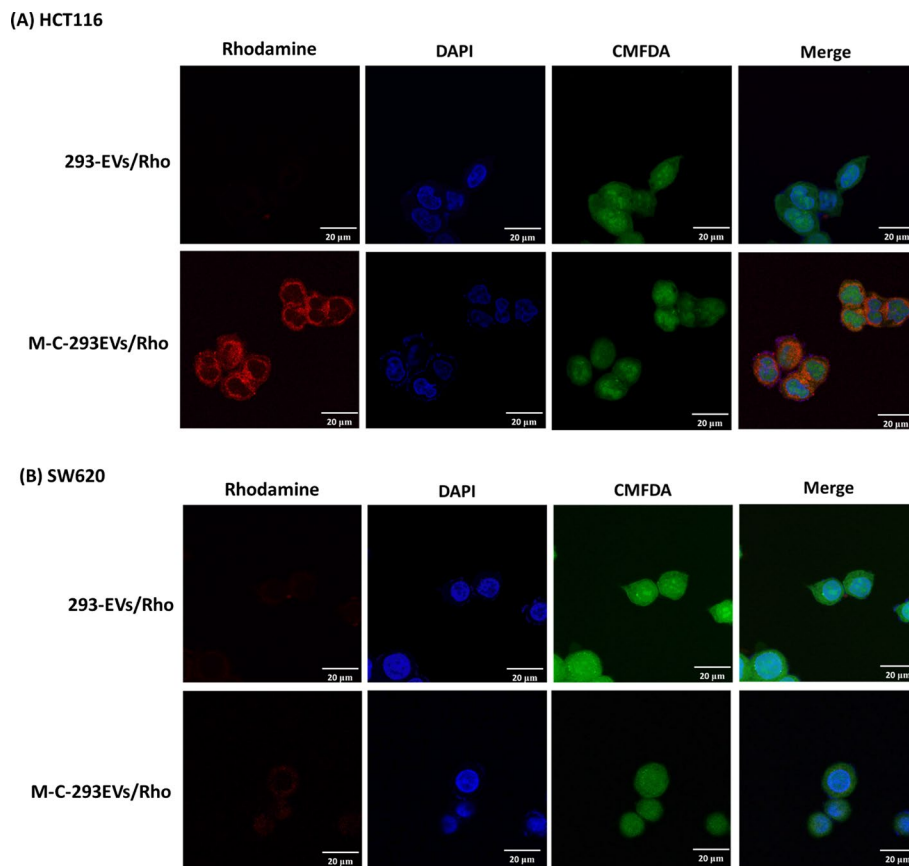


Fig. 3 Analysis of the specific accumulation of M-C-293EVs/Rho in colorectal cancer cell lines. 2 mg/ml of 293EVs/Rho and M-C-293EVs/Rho were added to HCT116 (EGFR +, **A**) or SW620 (EGFR-, **B**) cells and incubated for 60 min. The signal intensity of rhodamine B was analyzed using confocal microscopy. The excitation/emission spectra of rhodamine were 535/595–600 nm, and the excitation/emission spectra of DAPI were 358/461 nm. 293EVs/Rho: rhodamine-loaded 293EVs. M-C-293EVs/Rho: rhodamine-loaded M-C-293EVs

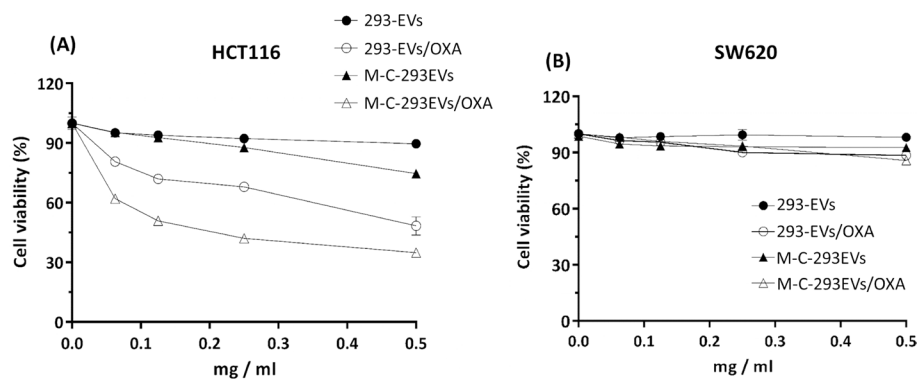


Fig. 4 Analysis of the cytotoxicity of M-C-293EVs in colorectal cancer cells. Serially diluted 293-EVs, 293-EVs/OXA, M-C-293EVs, or M-C-293EVs/OXA were used to treat HCT116 (**A**) and SW620 (**B**) cell lines. After 1 h of incubation, the culture medium was removed and replaced with fresh medium for an additional 48 h of incubation. Cell viability was analyzed using ATPlite. 293-EVs: extracellular vesicles from the HEK293 cell line; 293-EVs/OXA: oxaliplatin-loaded 293-EVs; M-C-293EVs: extracellular vesicles produced by the HEK293 cell line with a cetuximab-expressing membrane; M-C-293EVs/OXA: oxaliplatin-loaded M-C-293EVs

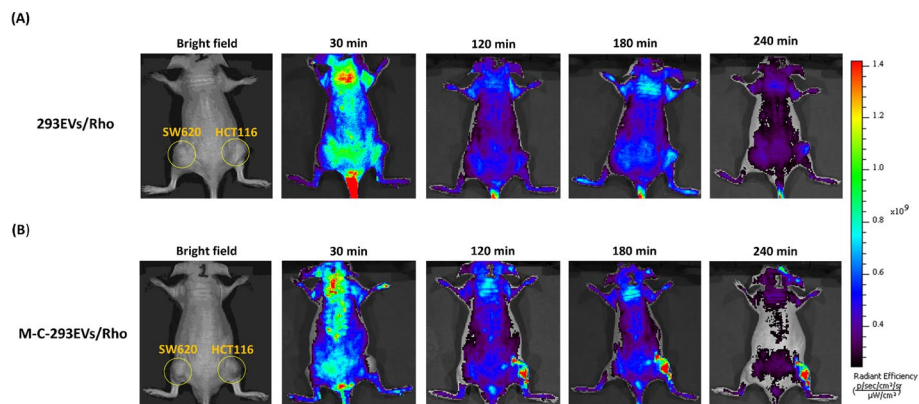


Fig. 5 Analysis of the specificity of accumulation of M-C-293EVs/Rho in a xenograft model. 2 mg/kg of 293EVs/Rho (**A**) and 2 mg/kg of M-C-293EVs/Rho (**B**) were separately injected into the tail veins of mice bearing SW620 tumors in the left leg and HCT116 tumors in the right leg. The accumulation of rhodamine (Em: 555 nm; Ex: 580 nm) was monitored at 30, 120, 180, and 240 min using fluorescent IVIS images. 293EVs/Rho: rhodamine-loaded 293EVs; M-C-293EVs/Rho: rhodamine-loaded M-C-293EVs

M-C-293EVs/Rho group, the fluorescence signal in the HCT116 tumor area reached 1.4×10^9 at 120, 180, and 240 min, whereas SW620 tumors did not exhibit this increase (Fig. 5B). These findings indicate that M-C-293EVs/Rho can specifically accumulate in EGFR + colorectal cancer in vivo.

M-C-293EVs/OXA enhance the efficacy of OXA against EGFR + colorectal cancer in vivo

To confirm that M-C-293EVs/OXA can enhance the efficacy of OXA against EGFR + colorectal cancer cells, we subcutaneously injected SW620 and HCT116 cells into the left legs of mice. Once the tumors reached a volume of 50 mm^3 , we administered PBS, 5 mg/kg/3 days (cumulative 3 doses) of oxaliplatin, M-C-293EVs, or M-C-293EVs/OXA. Tumor volume was measured every 3 days until day 30. The results showed that on day 30, the average tumor volumes in the HCT116 model for the PBS, OXA, M-C-293EVs, and M-C-293EVs/OXA groups were approximately 1121 mm^3 , 624 mm^3 , 752 mm^3 , and 438 mm^3 , respectively. Compared to PBS and M-C-293EVs, we found that M-C-293EVs alone could reduce tumor volume, indicating some therapeutic efficacy. Furthermore, M-C-293EVs/OXA showed enhanced efficacy compared to OXA alone (Fig. 6A). In the SW620 tumor model on day 30, the average tumor volumes for the PBS, OXA, M-C-293EVs, and M-C-293EVs/OXA groups were 852, 421, 841, and 537 mm^3 , respectively (Fig. 6B). Statistical analysis revealed no significant difference between PBS and M-C-293EVs ($p=0.875$) and no significant difference between OXA and M-C-293EVs/OXA ($p=0.193$). To further investigate tumor cell damage, we excised tumors on day 30 for H&E staining and apoptosis analysis. In the HCT116 tumors, the M-C-293EVs/OXA group had an average apoptosis area of 80%, significantly higher than the OXA group's 53% (Fig. 6C, E) ($p=0.035$). In the SW620 tumors, the M-C-293EVs/OXA group had an average apoptosis area of 33%, compared to the OXA group's 36%, with no significant difference (Fig. 6D, F) ($p=0.292$).

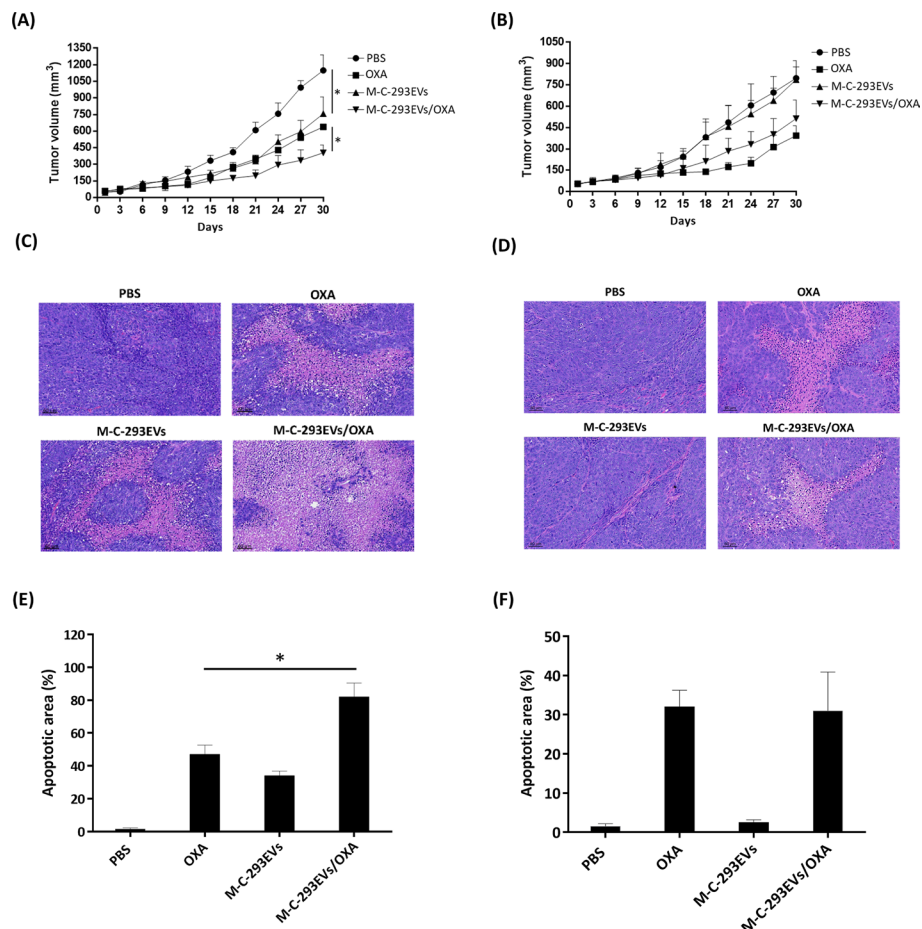


Fig. 6 Analysis of the specific efficacy of M-C-293EVs/Rho in a xenograft model. 2 mg/kg of OXA, M-C-293EVs, or oxaliplatin-encapsulating extracellular vesicles from the HEK293 cell line with cetuximab-expressing membrane (M-C-293EVs/OXA) were injected into the tail vein once every 3 days, for a total of three injections. The tumor volume was measured in the HCT116 (A) and SW620 (B) xenograft models. The mice were killed on day 30, and their tumors were stained with H&E (C, D) and subjected to statistical analysis (E, F). The values represent mean \pm SD, and asterisks indicate a significant difference ($*P < 0.05$). Light purple indicates areas of apoptosis

Materials and methods

Cell lines and cell culture

HEK293 cells are derived from human embryonic kidney cells, WI-38 cells are from human lung fibroblasts, PBMCs include lymphocytes and monocytes, HCT116 (EGFR+) is a human colorectal cancer cell line expressing EGFR, and SW620 (EGFR-) is a human colorectal cancer cell line lacking EGFR expression. (Bioresource Collection and Research Center, Hsinchu 300193, Taiwan) were cultured in Dulbecco's Modified Eagle Medium (Sigma-Aldrich, Darmstadt, Germany) supplemented with 10% bovine calf serum (Cytiva, Washington, USA) and 1% penicillin/streptomycin (Thermo Fisher Scientific Inc., Waltham, MA, USA). The cells were maintained in an incubator with 5% CO₂ at 37 °C.

Establishment of extracellular vesicles with membrane-expressed cetuximab (M-C-293EVs) and oxaliplatin (M-C-293EVs/OXA) encapsulation

The cetuximab light chain variable region (VL), light chain constant region kappa (CK), internal ribosome entry site (IRES), heavy chain variable region (VH), heavy chain constant region 1 (CH1), myc tag epitope (EQKLISEEDL), and cyto eB7 (Lin et al. 2017) were cloned into the pLKO_AS2 vector (National Core Facility for Biopharmaceuticals, Taipei, Taiwan) using NheI, AscI, BglII, and BstxI restriction enzymes. The plasmid was then transformed into TOP 10 cells (Thermo Fisher Scientific Inc, Waltham, USA) for amplification and extraction. The lentiviral vector was produced by co-transfecting pMD.G, pCMVΔR8.91 (National Core Facility for Biopharmaceuticals), and pLKO_AS2 cetuximab into HEK293 cells. Stable HEK293 cell lines that can secrete EVs with cetuximab-expressing membranes were selected using 1 µg/ml of neomycin sulfate (Thermo Fisher Scientific Inc, Waltham, USA) after infection with virus. The HEK293 cells were cultured in serum-free medium and treated with 5 mg/ml of oxaliplatin (Merck, Darmstadt, Germany) (Wang et al. 2023) and irradiated with UVB once at a dose of UVB, 300 J/m² for 1 h. The EVs with cetuximab-expressing membranes were collected from the cells (Ma et al. 2016).

Collection of EVs and western blot analysis

Collecting EVs from drug-treated or untreated cell lines involved a series of centrifugation steps. The conditioned medium from the cells was first centrifuged at 300 × g for 10 min at 4 °C to remove cellular debris. The supernatant was then subjected to further centrifugation at 2000 × g for 10 min at 4 °C to remove larger microvesicles. Next, the supernatant was centrifuged at 10,000 × g for 30 min at 4 °C to pellet smaller EVs. Finally, the pellet was resuspended in physiological saline and subjected to ultracentrifugation at 100,000 × g for 1.5 h at 4 °C to collect the extracellular vesicle pellet. For Western blot analysis, the collected EVs with cetuximab-expressing membranes, at 10 µg/well, were separated by SDS-PAGE and transferred onto a nitrocellulose NC membrane (Schleicher and Schuell, Einbeck, Germany). The NC membranes were probed with Mouse Anti-Human IgG Fab Antibody [HRP] (GenScript Biotech, Piscataway, NJ, USA), monoclonal HSP70 antibody (Thermo Fisher Scientific Inc, Waltham, USA), anti-CD81 antibody (abcam, Cambridge, UK), CD9 (abcam, Cambridge, UK), peroxidase-conjugated AffiniPure Goat Anti-Mouse IgG, Fc Fragment Specific (Jackson ImmunoResearch, West Grove, USA), or Rabbit Anti-Goat IgG Antibody, HRP conjugate (Thermo Fisher Scientific Inc, Waltham, USA), and visualized with the Immobilon Western Chemiluminescent HRP Substrate (Merck, Rahway, USA), according to the manufacturer's protocol.

Analysis of M-C-293EVs membrane-expressed antibodies, liquid chromatography–triple quadrupole mass spectrometry, transmission electron microscopy and nanoparticle tracking analysis

We used 2 mg of 293EVs and M-C-293EVs with CD9 Exosome Capture Beads (Abcam, Cambridge, UK), followed by staining with Anti-Human IgG (Fab specific)-FITC antibody (Thermo Fisher Scientific Inc., Waltham, USA) and fluorescence detection via LSRII flow cytometry (BD Biosciences, New Jersey, USA). We collected 5 mg/ml M-C-293EVs/OXA using liquid chromatography–triple quadrupole mass spectrometry

(LC–Q MS) to measure the OXA content. For all detection and quantification of analytes, we used the Waters ACQUITY UPLC system (Waters Corporation, Milford, MA) coupled with a tandem MS (Finnigan TSQ Quantum Ultra triple-quadrupole MS, Thermo Electron, San Jose, CA) in combination with the Xcalibur software (ThermoFinnigan, Bellefonte, PA). The LC–MS–MS system was equipped with an electrospray ion source (ESI) and was operated in positive mode. The injection volume was 10 μL on an ACQUITY UPLC BEH C18 Column (130 \AA , 1.7 μm , 2.1×50 mm, Waters Corporation, Milford, MA) equipped with a filter (Waters Acquity UPLC™ BEH C18 column, 1.7 μm , 2.1×5 mm) in front of the column. The flow rate was 200 $\mu\text{L}/\text{min}$, and the column temperature was 40 $^{\circ}\text{C}$. Solvents used were A: 0.1% acetic acid in water and B: 0.1% acetic acid in acetonitrile. The solvent programming was as follows: 0.0–1.0 min, 10% B; 7.0 min, 55% B; 7.1 min, 100% B; 7.1–8.0 min, 100% B; 8.1–12.0 min, 10% B. The MS–MS interface settings were as follows: spray voltage, 3000 V; sheath gas (N_2) pressure, 28 psi; auxiliary gas (N_2) pressure, 10 psi; capillary temperature, 350 $^{\circ}\text{C}$; collision gas (Ar) pressure, 1.0 mTorr.

Two micrograms of EVs were pipetted (5 μl) onto formvar-coated copper grids (FF200-Cu; Electron Microscopy Sciences, Hatfield, PA, USA) and allowed to settle for 20 min at room temperature. Excess phosphate-buffered saline (PBS) was removed by wicking with filter paper before fixation using a 2% paraformaldehyde, 2% glutaraldehyde, and 0.05 M phosphate solution for 2 min. Grids were washed three times with distilled water prior to application of 1% phosphotungstic acid counterstain for 1 min. Excess liquid was removed by wicking with filter paper, and the grids were allowed to dry overnight at room temperature. Grids were analyzed using a transmission electron microscope (Tecnai G2 20; FEI, Hillsboro, OR, USA). EVs were visualized and quantified using a nanoparticle tracking analyzer (Nanosight NS300; Nanosight Ltd., Amesbury, UK) with 70 mW laser with a wavelength of 405 nm. Urine samples were diluted in PBS at a ratio of 1:100, while serum samples were diluted at 1:1000. Duplicate measurements were recorded for each sample.

Analysis of rhodamine packaging by M-C-293EVs and confocal fluorescence microscope

After exosomes (EVs) were isolated from HEK293 cells or cell culture fluid transfected with membrane-expressing antibody plasmids. Next, the purified exosomes (5 mg/ml) were mixed with a rhodamine solution (10 mg/ml) and electroporated using the ECM-2001 Hybridoma System electroporation device (BTX, Connecticut, USA). The electroporation settings were 200 V pulse voltage, 3 s pulse time, and 2 pulses. After electroporation, the samples were incubated at 4 $^{\circ}\text{C}$ for 30 min to allow rhodamine to enter the exosomes. After incubation, the samples were centrifuged at $100,000 \times g$ for 10 min at 4 $^{\circ}\text{C}$ to remove rhodamine that had not entered the exosomes (Thery, et al. 2006; Dekkers, et al. 2008). The sample was then washed with PBS to separate the free rhodamine B and EVs by centrifugation at $100,000 \times g$ for 10 min at 4 $^{\circ}\text{C}$ in an ultracentrifuge (Optima™ XPN; Beckman Coulter, Brea, California, USA). The pellet was collected and resuspended in PBS for further use. Then, 2×10^3 SW620 and HCT116 cells were separately seeded on glass slides and 1, 2, 5 mg/ml M-C-293EVs/Rho was added to each cell culture and incubated for 60 min. The supernatant was removed and cells were washed with PBS. The cells were then fixed with 10% formalin (KINGFEX CO., LTD.,

Taipei, Taiwan) and stained with CellTracker™ Green CMFDA Dye (Thermo Fisher Scientific Inc.) and DAPI (Merck, Darmstadt, Germany) and mounted with mounting media (Thermo Fisher Scientific Inc.). Fluorescent images were acquired with a confocal fluorescence microscope (FV1000; Olympus, Tokyo, Japan).

Cell viability assay

Cells were plated in 96-well plates (2000 cells/well) overnight and serially diluted 293EVs, oxaliplatin-encapsulating EVs, EVs with cetuximab-expressing membranes, or oxaliplatin-encapsulating EVs with cetuximab-expressing membranes were added. Cell viability was detected using the ATPlite kit (510–17281; PerkinElmer, Chennai, India) and the luminescence value was measured using a multimode plate reader (VICTORTM X2; PerkinElmer).

Establishment of an ectopic cancer mouse model and analysis of the accumulation of rhodamine B-loaded extracellular vesicles with cetuximab-expressing membranes

Eight-week-old male nude mice (BALB/cAnN.Cg-Foxn1nu/CrlNarl) obtained from the National Laboratory Animal Center, Taiwan, were used in this study. The HCT116 and SW620 cell suspensions (2×10^6 in PBS) were subcutaneously inoculated into the right hind leg of the mice. Tumors were allowed to grow until they reached approximately 50 mm^3 in size. Rhodamine B-loaded EVs were injected into the tail vein at a dose of 5 mg/kg, and the accumulation of tumor fluorescence was measured at different time points using IVIS (PerkinElmer, Inc., Waltham, MA, USA).

Oxaliplatin-encapsulating extracellular vesicles with cetuximab-expressing membranes enhance the therapeutic effect of oxaliplatin on EGFR+ cancer cells

When the tumors reached approximately 50 mm^3 in size, mice were treated with PBS, oxaliplatin, EVs with cetuximab-expressing membranes, or oxaliplatin-encapsulating EVs with cetuximab-expressing membranes at a dose of 5 mg/kg by intraperitoneal injection every 3 days. Tumor size was measured every 2 days until the end of the experiment on day 30. The mice were then killed and the tumors were collected for observation. The tumor volume was calculated using the formula, tumor volume [mm^3] = (length (Zhang et al. 2020)) \times (width (Zhang et al. 2020))² \times 0.52. The Kaohsiung Medical University Institutional Animal Care and Use Committee approved this study (approval no. 112056). All experimental procedures were conducted in accordance with regulations. The tumor tissues were subjected to hematoxylin and eosin (HE) staining. For deparaffinization and rehydration, the slides were placed in xylene for 2–3 min, repeated twice, to remove paraffin. This was followed by rehydration through a graded series of ethanol solutions: 100, 95, and 70% ethanol for 2–3 min each. The slides were then rinsed in deionized water for 2–3 min. For hematoxylin staining, the slides were immersed in hematoxylin solution for 5–10 min. After staining, the slides were rinsed in running tap water for 5 min, then differentiated in 1% acid alcohol (1% HCl in 70% ethanol) for a few seconds. The slides were rinsed again in running tap water for 2 min and then blued in 0.2% ammonia water or saturated lithium carbonate solution for 1 min. A final rinse in running tap water for 5 min was performed. Subsequently, the slides were stained in eosin solution for 1–2 min and quickly rinsed in deionized water. For dehydration and

clearing, the slides were passed through 70, 95, and 100% ethanol for 1 min each, followed by two changes of xylene for 2 min each. Finally, the slides were mounted with a mounting medium and coverslips and then examined under a microscope (Olympus, Tokyo, Japan).

Discussion

In this study, we successfully established a stable system for secretion of EVs with cetuximab-expressing membranes and achieved passive encapsulation of oxaliplatin to form oxaliplatin-encapsulating EVs with cetuximab-expressing membranes. This approach maintained the particle size of the EVs. Furthermore, we confirmed that EVs with cetuximab-expressing membranes were specifically accumulated by EGFR+ cells, while EGFR- cells did not show this phenomenon. In the cytotoxicity experiments, we found that oxaliplatin-encapsulating EVs with cetuximab-expressing membranes exhibited significant cytotoxic effects on EGFR+ cells. Moreover, in the xenograft cancer animal model, we confirmed the specific accumulation of oxaliplatin-encapsulating EVs with cetuximab-expressing membranes in EGFR+ cells and significant enhancement of the therapeutic efficacy of oxaliplatin against EGFR+ cancer cells.

EVs are very suitable for incorporation with different anticancer agents to improve the efficacy of cancer therapy. Many studies have reported that EVs can carry a variety of different agents such as miRNA (Wang et al. 2020), siRNA (Walker et al. 2019), and chemotherapeutic drugs (Rezakhani et al. 2022; Lennaard, et al. 2021; Sutaria et al. 2017; Schindler et al. 2019) to target tumor for therapy, demonstrating that EVs have high compatibility with various drugs and can effectively enhance their half-life, stability, and tumor specificity. For example, Wang and colleagues loaded the miR-134 into exosomes to target and inhibit HER2 gene expression in breast cancer cells, thereby suppressing tumor growth. Experimental results showed that these miRNA exosomes significantly reduced the proliferation of breast cancer cells and promoted their apoptosis (Wang et al. 2020). In further studies used exosomes loaded with siRNA to specifically target and silence the KRAS G12D mutation gene. Their findings indicated that these siRNA-loaded exosomes efficiently suppressed the expression of the KRAS G12D mutation gene, leading to a marked reduction in tumor growth (Kosaka et al. 2019). Besides carrying RNA, EVs are also well-suited for delivering chemo-drugs. Dr. Schindler has successfully generated EVs carrying doxorubicin, which were rapidly taken up by cells. These EVs redistributed doxorubicin from the endoplasmic reticulum to the cytoplasm and nucleus, enhancing its efficacy against various cell lines. Importantly, unlike other delivery methods, EVs did not accumulate in the heart, potentially reducing cardiac side effects (Schindler et al. 2019). In our study, we further utilized antibodies to enhance the tumor selectivity of EVs. Our results showed that the OVA was effectively encapsulated by EVs, resulting in increased encapsulation rate and stability of OVA. In addition, *in vitro* (Fig. 4) and *in vivo* (Fig. 6) experiments demonstrated that EVs encapsulating oxaliplatin with cetuximab-expressing membranes were most effective in suppressing the growth of HCT116 tumors, but not SW480 tumors. Importantly, this approach showed superior therapeutic efficacy and reduced side effects compared to administering OVA alone. In summary, it is confirmed that EVs serve as a versatile

strategy for cancer drug delivery, offering broad drug encapsulation capability, enhanced stability, and tumor selectivity.

Enhancing the tumor specificity of EVs is crucial and effective in improving their clinical applications in cancer. EVs have the ability to penetrate various types of cells (Bahmani and Ullah 2022). These small lipid vesicles can transport their cargo of biomolecules, including proteins and nucleic acids, into recipient cells via mechanisms such as cell membrane fusion or internalization (Liu and Wang 2023; Kuipers et al. 2018; Skotland et al. 2020). However, EVs face several limitations in their application, such as rapid clearance, accumulation in the liver, and a lack of specificity towards specific targets (PMID: (Zhang et al. 2023; He et al. 2023; Yang et al. 2022)). Enhancing the tumor specificity of EVs through genetic engineering methods is highly important. For example, Yanhua Tian has demonstrated that the integration of the iRGD peptide as an exosomal targeting ligand than can provide KRAS siRNA carried EVs with a unique ability to precisely target and treat lung cancer (Tian et al. 2014; Limoni et al. 2019). Similarly, a study on HER2-positive breast cancer cells (SKBR3) used designed ankyrin repeat proteins as markers for EVs, combined with Tpd50 siRNA, to increase their targeted killing efficacy against breast cancer cells (Limoni et al. 2019). In addition, Zhang and colleagues employed glypican-3 (GPC3)-specific nanobody (HN3) and mouse single-chain IL-12 (mScIL12) modifications on EVs sourced from HEK293 cells to enhance their pharmacokinetic and biodistribution profiles, thereby enhancing their therapeutic efficacy against hepatocellular carcinoma (Zhang et al. 2023). These above studies indicate that EVs be easily genetically engineered to express various molecules, thus making them suitable for the treatment of different types of cancer. Notably, our study explored the application of oxaliplatin-loaded EVs expressing EGFR antibodies, demonstrating their potential to enhance targeted effects against colorectal cancer. Through FACS analysis (Fig. 2D), we determined that approximately 80% of M-C-293EVs highly expressed EGFR antibodies compared to control EVs. Additionally, confocal microscopy confirmed that M-C-293EVs accumulated significantly more in EGFR+ cells relative to control EVs (Fig. 3). In vivo IVIS imaging results (Fig. 5) further showed that M-C-293EVs, compared to control EVs, accumulated more extensively and for a longer duration (over 2 h) in EGFR+ HCT116 tumors, but not in EGFR- SW480 tumors, indicating that antibody expression can effectively enhance the specificity of EVs. Furthermore, animal treatment results demonstrated that the group treated with OXA-loaded M-C-293EVs could inhibit tumor growth more effectively than the clinical OXA (Fig. 6). Collectively, these findings highlight the potential of these modified EVs in enhancing targeted effects against colorectal cancer. This research provides significant insights into the precise targeting capabilities and multifunctional payload delivery of EVs in cancer treatment, establishing a solid foundation for the development of future cancer therapies.

Our EGFR-targeted M-C-293EVs might be broadly applied in the treatment of various cancers. Several clinically approved EGFR antibodies are utilized in cancer treatment, including cetuximab (Erbix), panitumumab (Vectibix), nimotuzumab, and necitumumab (Portrazza) (Cai et al. 2020; Sur et al. 2021). These antibodies are used to treat a wide variety of cancers, such as colorectal cancer, non-small cell lung cancer (NSCLC), head and neck squamous cell carcinoma (HNSCC), pancreatic cancer, glioblastoma and

breast cancer. This study has confirmed the effectiveness of EGFR-targeted M-C-293EVs in treating colorectal cancer. We are confident that by incorporating appropriate chemotherapy drugs, these EGFR-targeted M-C-293EVs can also be seamlessly extended to the treatment of other types of cancer. We considered that enhancing the drug encapsulation efficiency of our EGFR-targeted M-C-293EVs remains a challenge. We have tried various methods, but the encapsulation efficiency of oxaliplatin (OXA) has only reached about 1%, indicating there is substantial room for improvement in this area. In summary, we believe that EGFR-targeted M-C-293EVs carrying oxaliplatin (OXA) have several advantages. First, 293EVs are considered safe, as our experimental results have shown that 293EVs are non-toxic to various types of normal human cells (see supplementary Fig. 3). Second, our experiments demonstrate that EGFR-targeted M-C-293EVs exhibit specificity by accumulating specifically in tumors that express EGFR, whether tested *in vitro* or *in vivo*. Third, our EGFR-targeted M-C-293EVs could potentially be used broadly in the treatment of various cancers.

Supplementary Information

The online version contains supplementary material available at <https://doi.org/10.1186/s12645-024-00284-0>.

Supplementary Material 1.

Supplementary Material 2.

Supplementary Material 3.

Author contributions

Chih-Hung Chuang, A Chien, and Yi-Jung Huang: conceptualization, data curation, and formal analysis. Shang-Tao Chien, and Yi-Jung Huang: Funding acquisition, investigation, and project administration. Ming-Yii Huang, Yi-Ping Fang, Shi-Wei Chao, and Chia-Tse Li: methodology. Wun-Ya Jhang and Yun-Han Hsu: resources, software, and supervision. Shuo-Hung Wang: validation and visualization. Shang-Tao Chien, Yi-Jung Huang, and Chih-Hung Chuang: writing—original draft. Ming-Yii Huang, and Chih-Hung Chuang: writing—review and editing.

Funding

This study was financially supported by clinical research grants from Kaohsiung Armed Force General Hospital, Kaohsiung, Taiwan (No. MAB-112-802KB112577), the Ministry of Science and Technology, Taiwan (No. 110-2320-B-037-027-MY3, and No. 113-2314-B-037-064); the KMU-KMUH Co-Project of Key Research (No. KMU-DK(A)113017); and the Research Foundation (No. PT111001 and No. PT111002) of Kaohsiung Medical University, Taiwan. We thank the Drug Development and Value Creation Research Center, Kaohsiung Medical University, Taiwan, for instrumentation and equipment support.

Availability of data and materials

Data is provided within the manuscript or supplementary information files.

Declarations

Ethics approval and consent to participate

The Kaohsiung Medical University Institutional Animal Care and Use Committee approved this study (approval no. 112056). All experimental procedures were conducted in accordance with regulations.

Competing interests

The authors declare that they have no competing interests.

Author details

¹Department of Pathology, Kaohsiung Armed Forces General Hospital, No.2, Zhongzheng 1st Rd., Lingya Dist., Kaohsiung City 80284, Taiwan. ²Department of Nursing, Fooyin University, Kaohsiung, Taiwan. ³Department of Biochemistry, School of Post Baccalaureate Medicine, College of Medicine, Kaohsiung Medical University, No. 100 Shih-Chuan 1st Road, Kaohsiung, Taiwan. ⁴Drug Development and Value Creation Research Center, Kaohsiung Medical University, Kaohsiung, Taiwan. ⁵Department of Radiation Oncology, Kaohsiung Medical University Hospital, Kaohsiung Medical University, No 100 Shih-Chuan 1st Road, Kaohsiung 80708, Taiwan. ⁶Department of Radiation Oncology, School of Medicine, College of Medicine, Kaohsiung Medical University, Kaohsiung 80708, Taiwan. ⁷Center for Cancer Research, Kaohsiung Medical University, Kaohsiung 80708, Taiwan. ⁸School of Pharmacy, Kaohsiung Medical University, No. 100 Shih-Chuan 1st Road, Kaohsiung 80708, Taiwan. ⁹Regeneration Medicine and Cell Therapy Research Center, College of Medicine, Kaohsiung Medical University, Kaohsiung, Taiwan. ¹⁰Department of Medical Research, Kaohsiung Medical University Hospital, Kaohsiung Medical University, Kaohsiung, Taiwan. ¹¹Department of Medical Laboratory Science and Biotechnology, Kaohsiung Medical University, No 100 Shih-Chuan 1st Road, Kaohsiung, Taiwan.

Received: 19 April 2024 Accepted: 5 August 2024

Published online: 17 August 2024

References

- Bahmani L, Ullah M (2022) Different sourced extracellular vesicles and their potential applications in clinical treatments. *Cells*. <https://doi.org/10.3390/cells11131989>
- Cai WQ et al (2020) The latest battles between EGFR monoclonal antibodies and resistant tumor cells. *Front Oncol* 10:1249
- Chang WH, Cerione RA, Antonyak MA (2021) Extracellular vesicles and their roles in cancer progression. *Methods Mol Biol* 2174:143–170
- Chao MP, Weissman IL, Majeti R (2012) The CD47-SIRPalpha pathway in cancer immune evasion and potential therapeutic implications. *Curr Opin Immunol* 24(2):225–232
- Chen Z et al (2024) Encapsulation and assessment of therapeutic cargo in engineered exosomes: a systematic review. *J Nanobiotechnology* 22(1):18
- Cheng Q et al (2018) Reprogramming exosomes as nanoscale controllers of cellular immunity. *J Am Chem Soc* 140(48):16413–16417
- Dekkers R et al (2008) Gastrointestinal zygomycosis due to *Rhizopus microsporus var. rhizopodiformis* as a manifestation of chronic granulomatous disease. *Med Mycol* 46(5):491–4
- Fu P et al (2021) Extracellular vesicles as delivery systems at nano-/micro-scale. *Adv Drug Deliv Rev* 179:113910
- He C et al (2023) Engineered extracellular vesicles mediated CRISPR-induced deficiency of IQGAP1/FOXO1 reverses sorafenib resistance in HCC by suppressing cancer stem cells. *J Nanobiotechnology* 21(1):154
- Hou Y, Wang J, Wang J (2023) Engineered biomaterial delivery strategies are used to reduce cardiotoxicity in osteosarcoma. *Front Pharmacol* 14:1284406
- Kooijmans SAA et al (2016a) Modulation of tissue tropism and biological activity of exosomes and other extracellular vesicles: new nanotools for cancer treatment. *Pharmacol Res* 111:487–500
- Kooijmans SAA et al (2016b) PEGylated and targeted extracellular vesicles display enhanced cell specificity and circulation time. *J Control Release* 224:77–85
- Kosaka N et al (2019) Exploiting the message from cancer: the diagnostic value of extracellular vesicles for clinical applications. *Exp Mol Med* 51(3):1–9
- Kuipers ME et al (2018) Pathogen-derived extracellular vesicle-associated molecules that affect the host immune system: an overview. *Front Microbiol* 9:2182
- Lennaard AJ et al (2021) Optimised electroporation for loading of extracellular vesicles with doxorubicin. *Pharmaceutics*. <https://doi.org/10.3390/pharmaceutics14010038>
- Li Y et al (2018) A33 antibody-functionalized exosomes for targeted delivery of doxorubicin against colorectal cancer. *Nanomedicine* 14(7):1973–1985
- Limoni SK et al (2019) Engineered exosomes for targeted transfer of siRNA to HER2 positive breast cancer cells. *Appl Biochem Biotechnol* 187(1):352–364
- Lin WW et al (2017) Enhancement effect of a variable topology of a membrane-tethered anti-poly(ethylene glycol) antibody on the sensitivity for quantifying PEG and PEGylated molecules. *Anal Chem* 89(11):6082–6090
- Liu YJ, Wang C (2023) A review of the regulatory mechanisms of extracellular vesicles-mediated intercellular communication. *Cell Commun Signal* 21(1):77
- Liu X, Xiao C, Xiao K (2023) Engineered extracellular vesicles-like biomimetic nanoparticles as an emerging platform for targeted cancer therapy. *J Nanobiotechnology* 21(1):287
- Ma J et al (2016) Reversing drug resistance of soft tumor-repopulating cells by tumor cell-derived chemotherapeutic microparticles. *Cell Res* 26(6):713–727
- Rahbarghazi R et al (2019) Tumor-derived extracellular vesicles: reliable tools for cancer diagnosis and clinical applications. *Cell Commun Signal* 17(1):73
- Rezakhani L et al (2022) Exosomes: special nano-therapeutic carrier for cancers, overview on anticancer drugs. *Med Oncol* 40(1):31
- Schindler C et al (2019) Exosomal delivery of doxorubicin enables rapid cell entry and enhanced in vitro potency. *PLoS ONE* 14(3):e0214545
- Shi X et al (2020) Genetically engineered cell-derived nanoparticles for targeted breast cancer immunotherapy. *Mol Ther* 28(2):536–547
- Skotland T et al (2020) An emerging focus on lipids in extracellular vesicles. *Adv Drug Deliv Rev* 159:308–321
- Somiya M, Yoshioka Y, Ochiya T (2018) Biocompatibility of highly purified bovine milk-derived extracellular vesicles. *J Extracell Vesicles* 7(1):1440132
- Stridfeldt F et al (2023) Analyses of single extracellular vesicles from non-small lung cancer cells to reveal effects of epidermal growth factor receptor inhibitor treatments. *Talanta* 259:124553
- Sur D et al (2021) A critical review of second-generation anti-EGFR monoclonal antibodies in metastatic colorectal cancer. *Curr Drug Targets* 22(9):1034–1042
- Sutaria DS et al (2017) Achieving the promise of therapeutic extracellular vesicles: the devil is in details of therapeutic loading. *Pharm Res* 34(5):1053–1066
- Thery C et al (2006) Isolation and characterization of exosomes from cell culture supernatants and biological fluids. *Curr Protoc Cell Biol*. <https://doi.org/10.1002/0471143030.cb0322s30>
- Tian Y et al (2014) A doxorubicin delivery platform using engineered natural membrane vesicle exosomes for targeted tumor therapy. *Biomaterials* 35(7):2383–2390
- Tian J et al (2023) Engineered exosome for drug delivery: recent development and clinical applications. *Int J Nanomedicine* 18:7923–7940

- Walker S et al (2019) Extracellular vesicle-based drug delivery systems for cancer treatment. *Theranostics* 9(26):8001–8017
- Wang J et al (2020) MiR-4443 promotes migration and invasion of breast cancer cells by inhibiting PEBP1 expression. *Nan Fang Yi Ke Da Xue Xue Bao* 40(12):1712–1719
- Wang L et al (2023) Extracellular vesicles for drug delivery in cancer treatment. *Biol Proced Online* 25(1):28
- Wu P et al (2021) Extracellular vesicles: a bright star of nanomedicine. *Biomaterials* 269:120467
- Yang C et al (2022) Glioma-derived exosomes hijack the blood–brain barrier to facilitate nanocapsule delivery via LCN2. *J Control Release* 345:537–548
- Zeng Y et al (2022) Biological features of extracellular vesicles and challenges. *Front Cell Dev Biol* 10:816698
- Zhang LY et al (2020) Membrane derived vesicles as biomimetic carriers for targeted drug delivery system. *Curr Top Med Chem* 20(27):2472–2492
- Zhang J et al (2023) Surface engineering of HEK293 cell-derived extracellular vesicles for improved pharmacokinetic profile and targeted delivery of IL-12 for the treatment of hepatocellular carcinoma. *Int J Nanomedicine* 18:209–223
- Zhu LP et al (2018) Hypoxia-elicited mesenchymal stem cell-derived exosomes facilitates cardiac repair through miR-125b-mediated prevention of cell death in myocardial infarction. *Theranostics* 8(22):6163–6177

Publisher's Note

Springer Nature remains neutral with regard to jurisdictional claims in published maps and institutional affiliations.